Available online at www.sciencedirect.com
SCIENCE DIRECT
Journal of volcanology and geothermal research
ELSEVIER
Journal of Volcanology and Geothermal Research 152 (2006) 331–346
www.elsevier.com/locate/jvolgeores

Incorporating seismic observations into 2D conduit flow modeling

L. Collier, J. Neuberg *

Department of Earth Sciences, University of Leeds, Leeds, UK

Received 15 June 2005; received in revised form 7 October 2005; accepted 16 November 2005
Available online 18 January 2006

Abstract

Conduit flow modeling aims to understand the conditions of magma at depth, and to provide insight into the physical processes that occur inside the volcano. Low-frequency events, characteristic to many volcanoes, are thought to contain information on the state of magma at depth. Therefore, by incorporating information from low-frequency seismic analysis into conduit flow modeling a greater understanding of magma ascent and its interdependence on magma conditions and physical processes is possible. The 2D conduit flow model developed in this study demonstrates the importance of lateral pressure and parameter variations on overall magma flow dynamics, and the substantial effect bubbles have on magma shear viscosity and on magma ascent. The 2D nature of the conduit flow model developed here allows in depth investigation into processes which occur at, or close to the wall, such as magma cooling and brittle failure of melt. These processes are shown to have a significant effect on magma properties and therefore, on flow dynamics. By incorporating low-frequency seismic information, an advanced conduit flow model is developed including the consequences of brittle failure of melt, namely friction-controlled slip and gas loss. This model focuses on the properties and behaviour of magma at depth within the volcano, and their interaction with the formation of seismic events by brittle failure of melt.

Keywords: magma; low-frequency seismic events; modelling; brittle failure

1. Introduction

The style of volcanic eruptions, whether explosive or effusive, is directly linked to the physical processes and conditions occurring at depth within the volcano. It is these processes that conduit flow models attempt to recreate, to obtain further insight into eruption styles and magma properties. Conduit flow modeling, therefore, requires an accurate description of both fluid mechanics and magma properties (Fig. 1).

Magma conduit flow was first modeled by Wilson et al. (1980) who made a number of simplifying assumptions, such as averaging flow properties at each depth (1D), and neglecting viscosity changes with depth. Subsequent work has extended significantly the processes and conditions investigated by conduit models, including, for example, variations in viscosity (Mastin and Ghiorso, 2000; Melnik and Sparks, 1999; Papale and Dobran, 1993), fragmentation processes (Dobran, 1992; Mastin and Ghiorso, 2000; Papale et al., 1998), crystal growth (Melnik and Sparks, 1999, 2002) and adiabatic temperature changes (Buresti and Casarosa, 1989; Mastin, 1995).

All of the conduit models mentioned above make the underlying assumption that flow properties can be averaged across the conduit at each depth, i.e. modeling in one dimension. While this assumption seems justified given the large length of conduits compared to their width, the analytical expressions of Massol and Jaupart

* Corresponding author. Fax: +44 113 343 5259.
E-mail address: locko@earth.leeds.ac.uk (J. Neuberg).

0377-0273/$ - see front matter © 2005 Elsevier B.V. All rights reserved.
doi:10.1016/j.jvolgeores.2005.11.009

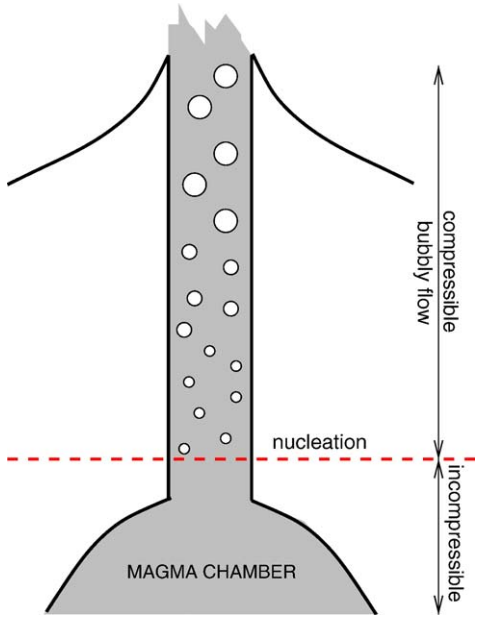

Fig. 1. Sketch of the volcanic conduit system during an effusive eruption where fragmentation is not achieved and the highly viscous magma is extruded from the conduit as a spine or a dome.

(1999) and the 2D compressible models of Massol et al. (2001) indicate that significant lateral variations of magma properties can develop, altering overall flow behaviour.

Within this paper, a 2D conduit flow model is developed using a Finite Element Method (FEM) to explore further the effects of lateral parameter variations on overall flow dynamics, and to investigate the conditions of magma at all positions within the conduit. The 2D nature of the model enables processes to be explored which occur close to, or at, the conduit wall, such as magma cooling and fracturing of melt. Furthermore, the effect these processes may have on the overall flow behaviour of magma within volcanic conduits can be fully explored.

One of the main aims of this paper is to incorporate seismic observations into conduit flow modeling to enable further understanding into the physics of magma conditions and flow at depth. Key volcanic seismic events are the so-called low-frequency events, observed at many silicic volcanoes including Redoubt, Alaska (Stephens et al., 1994) and Soufrière Hills, Montserrat (Miller et al., 1998). Lahr et al. (1994) further subdivided this group into *long period* and *hybrid* events, though both event types have the characteristic low frequency content and therefore, within this study will be collectively referred to as low-frequency (LF) events. These events contain information on processes which are occurring at depth in volcanic conduits, and are therefore key observations to consider when modeling magma flow at depth. By combining the disciplines of seismic analysis and magma flow modeling a greater insight into the state of magma at depth can be inferred than from each discipline alone. Specifically, the possibility of melt reacting in a brittle manner and fracturing at localised points within magma conduits, releasing seismic energy 3 producing observed seismic events is studied (Goto, 1999; Tuffen et al., 2003; Neuberg et al., in press). An advanced conduit model is developed that includes the proposed consequences of brittle failure of melt, friction-controlled slip and gas loss, such that the effect of these mechanisms on the overall magma flow dynamics and eruption style can be fully explored.

2. 2D compressible flow dynamics

2.1. Governing equations

Magma flow is modeled using the Navier-Stokes equation. Silicic magma is observed to be compressible due to its gas content, and its viscosity can vary over several orders of magnitude within conduits, and cannot be assumed to be constant (Bagdassarov and Dingwell, 1993). However, magma flow can be assumed to be steady and laminar, thus the inertial terms are neglected. Therefore, the equation of motion is,

$$-\nabla P+\nabla\cdot\eta_{\mathrm{b}}\left(\nabla\mathbf{U}+(\nabla\mathbf{U})^{T}\right)+\nabla\lambda(\nabla\cdot\mathbf{U})-\rho_{\mathrm{b}}\mathbf{g}=0, \tag{1}$$

and the compressible continuity equation,

$$\nabla\cdot(\rho_{\mathrm{b}}\mathbf{U})=0. \tag{2}$$

Here λ is the second coefficient of viscosity, which can be alternatively expressed as $\zeta_{\mathrm{b}}-2\eta_{\mathrm{b}}/3$, where ζ_{b} and η_{b} are the volume and shear viscosities of the magma, respectively. ρ_{b} is the density of the bulk magma, and $\mathbf{U}=(u, v)$ is the velocity vector field of the flow.

The bulk magma is assumed to consist of a mixture of melt, crystals and gas bubbles. However, it is assumed that the bulk properties of the magma are averages of these three individual phases weighted by their volume fraction. Bulk magma properties are labeled with the subscript ‘b’, melt properties with ‘m’, gas properties with ‘g’, and crystal properties with ‘c’. Therefore, the density of the melt and crystal mixture is given by,

$$\rho_{\mathrm{m+c}}=\rho_{\mathrm{m}}(1-\chi_{\mathrm{c}})+\rho_{\mathrm{c}}\chi_{\mathrm{c}}, \tag{3}$$

Table 1
Parameters and constants used, chosen to represent silicic magma, specifically Soufri'ere Hills magma. The ranges indicate the parameters used within the sensitivity analysis and the values in brackets are the default values used, unless otherwise stated

Parameter	Value	Reference
Melt density, ρ_m	2200–2400 (2300) kg m^{-3}	Rivers and Carmichael (1987)
Crystal density (An_{53}), ρ_c	2680 kg m^{-3}	Carmichael (1990)
Crystal content, χ_c	30–40 (30)%	Devine et al. (1998)
Rock density, ρ_r	2300–2700 kg m^{-3}	Melnik and Sparks (2002)
Magma temperature, T	1090–1150 (1120) K	Devine et al. (1998)
Total H_2O conc., c_o	0.037–0.048 (0.0425)	Barclay et al. (1998)
Excess chamber pressure, P_{ch}	0–20 (10) MPa	Sparks (1997)
Temp. di erence, ΔT	100–200 (150) K	Section 3
Surface tension, Γ	0.05 N m^{-1}	Lyakhovsky et al. (1996)
Solubility constant, K_h	4.11×10^{-6}	Shaw (1974)
Bubble radius, R	10^{-7}–10^{-4} m	Eq. (7)
Bubble. no. density, n	10^{12} m^{-3}	Hurwitz and Navon (1994)
Gas density, ρ_g	50–300 kg m^{-3}	Eq. (5)
Mol. weight of water, M	0.018 kg mol^{-1}	General constant
Ideal gas const., C_g	8.314 J $mol^{-1}K^{-1}$	General constant
Conduit radius/half-width, a	15 m	Sparks et al. (2000)
Magma chamber depth, L	5000 m	Barclay et al. (1998)
Melt shear viscosity, η_m	10^4–10^8 Pa s	(Hess and Dingwell, 1996)
Magma shear viscosity, η_b	10^3–10^6 Pa s	calculated
Melt heat capacity, C_p^m	1604 J (K kg)$^{-1}$	Spera (2000)
Gas heat capacity, C_p^g	30 J (K kg)$^{-1}$	Ideal gas
Magma heat capacity, C_p^b	1132 J (K kg)$^{-1}$	$C_p^m(1-\chi_g)+C_p^g\chi_g$
Rock heat capacity, C_p^r	800 J (K kg)$^{-1}$	Gu'eguen and Palciauskas (1994)
Melt conduct., k_m	1.04 W (m K)$^{-1}$	Murase and McBirney (1973)
Gas conduct., k_g	0.07 W (m K)$^{-1}$	Gu'eguen and Palciauskas (1994)
Magma conduct., k_b	0.35/0.67 W (m K)$^{-1}$	min/max Hashin-Shrikman bounds
Rock conduct., k_r	2.25 W (m K)$^{-1}$	Gu'eguen and Palciauskas (1994)
Permeability, K	10^{-12} m^2	Melnik and Sparks (2002)
Friction coeff., β	5×10^6 Pa s m^{-1}	–

where χ_c is the volume fraction of crystals w.r.t. the melt and crystal mixture, which is taken to be constant (Table 1). ρ_m and ρ_c are the densities of the melt and crystal phases, respectively. Hence, the density of the bulk magma (melt, crystals and gas) is given by,

$$\rho_b = \rho_{m+c}(1-\chi_g) + \rho_g\chi_g. \quad (4)$$

Here χ_g is the volume fraction of gas w.r.t. the bulk magma, and ρ_g is the gas density which is determined through the ideal gas law,

$$\rho_g = \frac{MP}{C_gT}, \quad (5)$$

with M as the molecular weight of water, T as the magma temperature and C_g as the ideal gas constant (Table 1).

Within the magma the concentration of water dissolved within the melt at any particular pressure is given by Henry's solubility law,

$$c_m = K_hP^n, \quad (6)$$

where $K_h=4.11\times10^{-6}$ $Pa^{-1/2}$ is the solubility constant and $n=1/2$, both calibrated experimentally for a rhyolitic melt at low pressures with water as the only volatile in the system (Shaw, 1974). As depth decreases, pressure reduces allowing water to exsolve out of the melt and form gas bubbles, which then increase in size with decreasing depth as more water comes out of solution (Navon et al., 1998),

$$R^3 = \frac{S_0^3\rho_m(c_0-c_m)}{\rho_g}. \quad (7)$$

where R is the bubble radius, S_0 is the initial size of the melt shell determined from the bubble number density, n, which is assumed to be constant (Table 1),

$$S_0^3 = \frac{3}{4\pi n}, \quad (8)$$

with c_0 as the initial water content within the melt. This increase in bubble size with decreasing depth and pressure causes an increase in gas volume fraction (χ_g) and therefore, a decrease of density of the bulk magma (Eq. (4)).

Other parameters to be solved for the flow of magma are the volume and shear viscosities of the magma. The volume viscosity of the magma (ζ_b) is determined simply through the gas volume fraction (Prud'Homme and Bird, 1978),

$$\zeta_b = \frac{4}{3}\frac{\eta_{m+c}(1-\chi_g)}{\chi_g}, \quad (9)$$

where η_{m+c} is the shear viscosity of the melt and crystal mixture. The shear viscosity of the melt is dependent on the magma temperature, T, and the concentration of water dissolved within the melt, c_m (Eq. (6)). Hess and Dingwell (1996) developed an empirical expression for the shear viscosity of rhyolitic melt which is used throughout this study. The inclusion of solid crystals acts to increase shear viscosity, and for crystal contents <40% this effect can be represented by the Einstein-Roscoe equation,

$$\eta_{m+c} = \eta_m\left(1-\frac{\chi_c}{\chi_c^{max}}\right)^{-2.5}, \quad (10)$$

where χ_c^{max} is the volume fraction of crystals at which maximum packing is achieved, $\chi_c^{max} \approx 0.6$, (Marsh, 1981). In a similar fashion, the presence of gas bubbles also has an effect on the bulk shear viscosity of magma flow (Llewellin et al., 2002; Manga and Loewenberg, 2001; Stein and Spera, 2002). Gas bubbles have been observed experimentally to increase or decrease with shear viscosity, depending on their deformation (Bagdassarov and Dingwell, 1993; Stein and Spera, 1992). A spherical, undeformed bubble causes the flow to move around the bubble and increases the viscosity of the magma. However, if the bubbles are deformed and elongated due to flow and high strain rates, the increased surface area of the bubbles allows slip to occur, decreasing the bulk shear viscosity of the magma (Manga et al., 1998). The capillary number (C_a) indicates which regime the magma system is in,

$$C_a = \frac{\eta_m R\dot{\varepsilon}}{\Gamma}, \quad (11)$$

where $\dot{\varepsilon}$ is the strain rate of the magma flow, R is the undeformed bubble radius, and Γ is the surface tension of the bubbles. When $C_a<1$, the bubbles are undeformed, and the shear viscosity of the magma is increased. Whereas, when $C_a>1$, the elongated, deformed bubbles decrease the magma shear viscosity. Within the model developed here, the 'minimum variation' suggested by Llewellin and Manga (2005) is applied:

$$\text{If } C_a<1:\ \eta_{rel} = (1-\chi_g)^{-1} \quad (12)$$

$$\text{If } C_a>1:\ \eta_{rel} = (1-\chi_g)^{5/3}. \quad (13)$$

Here $\eta_{rel}=\eta_b/\eta_{m+c}$, is the viscosity of the magma, relative to the viscosity of the melt and crystal mixture (η_{m+c}) (Eq. (10)).

In this way, the viscosities of the magma are modeled to be dependent on the melt, crystal and bubble phases and content. The input parameters and constants used in the conduit flow models are listed in Table 1. Values are chosen to represent, as closely as possible, the magma of Soufrière Hills Volcano, and where single values cannot be justified, an entire range is given, consistent with silicic magma.

2.1.1. Gas loss theory

Magma conduit models are generally assumed to be *closed*, hence, no gas is lost from the conduit system. However, it is generally accepted that gas is lost from magma conduits and volcanic systems, as steam and gas is observed to escape at volcanic domes, e.g. at Soufrière Hills Volcano (Edmonds et al., 2003; Sparks et al., 2000). From field observations it seems also clear that gas is lost from magma conduits (Eichelberger et al., 1986; Stasiuk et al., 1996), though the exact mechanism for this loss is not fully understood. Here the 2D conduit flow model is extended to include gas loss, i.e. an *open* conduit.

Gas loss within the models is assumed to occur horizontally through the conduit wall into the surrounding country rock, helped by the formation of fractures and cracks, as proposed by Jaupart and Allègre (1991) and Jaupart (1998). At each depth the gas volume fraction is determined by considering the amount of gas exsolved from the melt and the amount of gas lost into the surrounding country rock.

$$\frac{\partial\chi_g}{\partial z} = (1-\chi_g)^2\frac{\rho_m}{\rho_g}\left[\frac{\partial_P}{\partial_z}\left(\frac{\chi_g}{\rho_m(1-\chi_g)}\frac{M}{C_g T}+1/2c_m\right) - \frac{2q_g}{q_m a}\right], \quad (14)$$

where q_m is the flux of the melt. The degree of gas lost from the magma, q_g, is determined through Darcy's Law (Jaupart and Allègre, 1991),

$$q_g = P_{drive}K_{eff}\chi_g\rho_g, \quad (15)$$

which depends on the effective permeability of the magma and country rock (K_{eff}; Table 1) and the surrounding country rock and the driving pressure (P_{drive}), which is defined as the difference between magma pressure and the lithostatic country rock pres-

sure. The effective permeability (K_{eff}) is dependent on the permeability of the rock/magma (K), the viscosity of the gas (η_g), and a length scale, L, taken as the typical distance for the pressure decrease, P_{drive}, to occur,

$$K_{eff} = \frac{K}{\eta_g L}. \quad (16)$$

This theory of Jaupart (1998) is extended to allow for 2-dimensions, by considering the extra distance gas from the centre of the conduit is required to travel before it is considered 'lost' (i.e. in L). This implies that within the 2D conduit models, more gas is expected to be lost from the conduit wall than from the centre of the conduit.

Within the FEM conduit flow models, by setting the horizontal gas flux to zero, no gas is lost from the system and therefore, the conduit model is *closed*. Whereas by allowing the gas flux to be non-zero, gas is lost from the system and the conduit model is *open* (with parameters as in Table 1). The advantage of this flexibility is that gas loss can be included for the whole conduit length, or only at certain depths, and the effect on magma flow and therefore, the eruption style at the surface can be studied.

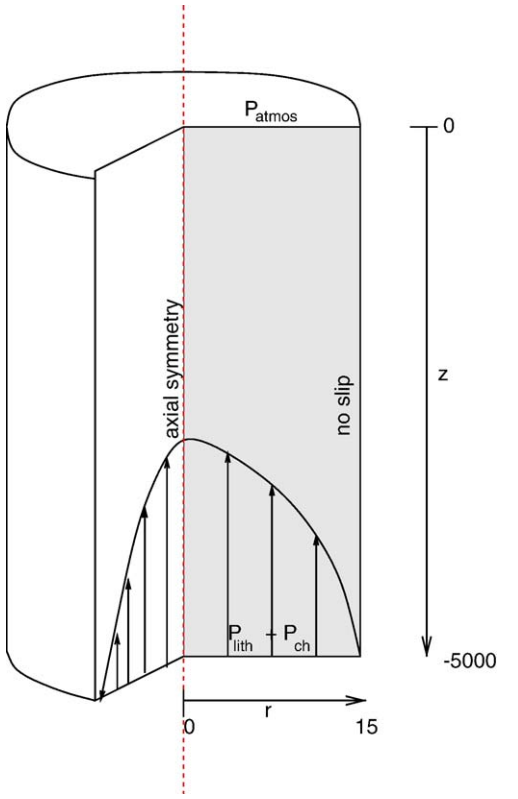

Fig. 2. Schematics of the conduit model, taken to be a cylindrical pipe assuming axial symmetry (shaded area). Boundary conditions and dimensions are as marked.

2.2. Boundary conditions

The conduit flow model is set up as shown in Fig. 2, assuming a cylindrical geometry with constant radius, a=15 m (Sparks et al., 2000; Watts et al., 2002). The length of the conduit is taken to be 5000 m, extending from the magma chamber depth to the surface (Barclay et al., 1998).

The magma ascent is driven by a pressure gradient set-up by the boundary conditions at the magma chamber depth and at the conduit exit. At the magma chamber depth the pressure is set to equal the lithostatic country rock pressure (P_{lith}) plus a certain excess chamber pressure (P_{ex}), and at the conduit exit the pressure (normal stress) is taken to be equal to the atmospheric pressure (P_{atmos}). This upper boundary condition is taken to represent magma being extruded from the conduit forming spines which are continuously eroding due to gravitational collapse. No dome above the conduit is assumed.

The range of possible values for the excess chamber pressure is estimated from the strength of the country rock surrounding the magma conduit. Sparks (1997) suggests ranges of 5–20 MPa for Soufrière Hills Volcano, and Stasiuk et al. (1993) estimated excess chamber pressures of 10–23 MPa for Lonquimay 10 Volcano, Chile. In this study a range of flow behaviours with P_{ex}=0–20 MPa is investigated (Table 1). The model is assumed to be axial symmetric such that the region required to be modeled can be reduced to the shaded area (Fig. 2).

The conduit wall is the boundary between the flowing viscous magma and the stationary solid rock. The standard boundary conditions for Newtonian fluids is *no slip*, i.e. $\mathbf{U}=(u, v)=0$ at the wall. However, it is likely in magma conduits that fracturing at the conduit wall would allow friction-controlled slip to occur. The 2D conduit flow models developed here have been extended to incorporate this boundary condition, i.e. allowing for a finite magma flow velocity at the wall dependent on the degree of friction, by using the Navier slip condition (Lamb, 1945),

$$-\eta_b \frac{\partial v}{\partial \gamma} = \beta v, \quad (17)$$

and

$$u = 0. \quad (18)$$

Here β is the friction coefficient (Table 1), alternatively defined as,

$$\beta = \frac{\eta_b}{L}, \tag{19}$$

where L is the slip distance. Hence, it is possible to explore the effects of such boundary conditions on magma properties at depth in the volcano and the overall flow dynamics.

2.3. Model summary

The previous sections list the key equations solved for within the 2D conduit flow models. The models are solved using Finite Element Methods through the software package FEMLAB from Comsol (www.uk.comsol.com). Within FEMLAB the geometry of the model is first assigned then a non-regular, triangular mesh is applied which allows an accurate representation of the geometry. The mesh is non-adaptive and typically contains 9 elements across the conduit and around 600 along the conduit length. The entire model consists of 5520 elements and 38306 degrees of freedom. The fundamental equations governing flow and magma properties (Eqs. (1)–(13)) are non-dimensionalised and solved simultaneously within FEMLAB applying the relevant boundary conditions (Section 2.2)). Models were run with different mesh resolutions to check the numerical convergence of the models.

2.4. Compressible flow parameters

First, to illustrate compressible flow dynamics, the variation of magma properties with depth and lateral position is investigated. The 2D conduit flow model is set with *no slip* boundary condition at the conduit wall and gas loss is excluded such that the magmatic system is considered *closed*.

2.4.1. Parameter variations with depth

Parameters, such as the dissolved water content, the gas volume fraction and the magma shear viscosity, depend directly on the pressure (e.g. Eq. (6)), and therefore, vary with depth. The values of these parameters have a strong 12 influence on the overall flow characteristics of the magma, and therefore, on the eruptive style.

Gas is observed to be exsolved at depths 3000–3500 m, and this 'nucleation depth' decreases as the excess chamber pressure is increased (P_{ch}) due to the corresponding rise in pressure at this depth (Fig. 3(a)). Further gas is exsolved as the magma rises (decreasing depth), causing a corresponding decrease in magma density and increase in magma flow velocity, due to mass conservation (Fig. 3).

Within these *closed* conduit models, the gas volume fraction at the conduit exit is observed to be unreasonable high (Fig. 3(c)). It is thought that above gas volume fractions of 75% magma fragments, however such mechanisms are beyond the scope of our models. These high values are obtained due to the assumption of a *closed* conduit system. In later sections, the inclusion of gas loss reduces the gas volume fraction to more reasonable values. The high gas volume fractions within this model also increase the flow rate of magma through the conduit, as illustrated in Fig. 3(b). Typical average flow velocities modeled are 0.1–0.5 m s^{-1}, with the flow increasing to around 1 m s^{-1}at the conduit exit. Estimated ascent rates from petrological studies suggest that Soufrière Hills Volcano magma rises at the speed of 0.001–0.01 m s^{-1}(Rutherford and Gardner, 2000). These observations are noticeably lower than those modeled here, however it will be seen in later sections that by including gas loss within an *open* conduit the magma ascent rates are reduced to more realistic values.

The shear viscosity of the melt increases steadily as depth is decreased in the conduit (Fig. 3(e)), as the dissolved water content in the melt decreases 13 (Hess and Dingwell, 1996). At shallow depths this variation is rapid, causing the melt to be highly viscous (around 10^8 Pa s). Over the entire conduit length the melt shear viscosity is seen to increase by around 3 orders of magnitude. The shear viscosity of the magma, however, only varies over one order of magnitude with depth (Fig. 3(f)). The shear viscosity of the magma is less than that of the melt as the capillary number (C_a) is greater than one, indicating the high degree of bubble deformation due to the flow rate, causing a viscosity decrease. The variation of magma shear viscosity with depth is more complicated than that of the melt shear viscosity due to several factors controlling it: in general, magma shear viscosity increases with decreasing depth, due to the effect of the melt shear viscosity, but this factor is reduced by the elongated, deformed bubbles (Llewellin and Manga, 2005). At very shallow depths (in the upper few hundred metres) the shear viscosity of the magma is observed to decrease suddenly. This is due to the effect of the elongated bubbles becomes dominant over the effect of the melt shear viscosity.

2.4.2. Lateral parameter variations

Massol and Jaupart (1999) predicted that by including compressibility, lateral variations in pressure would

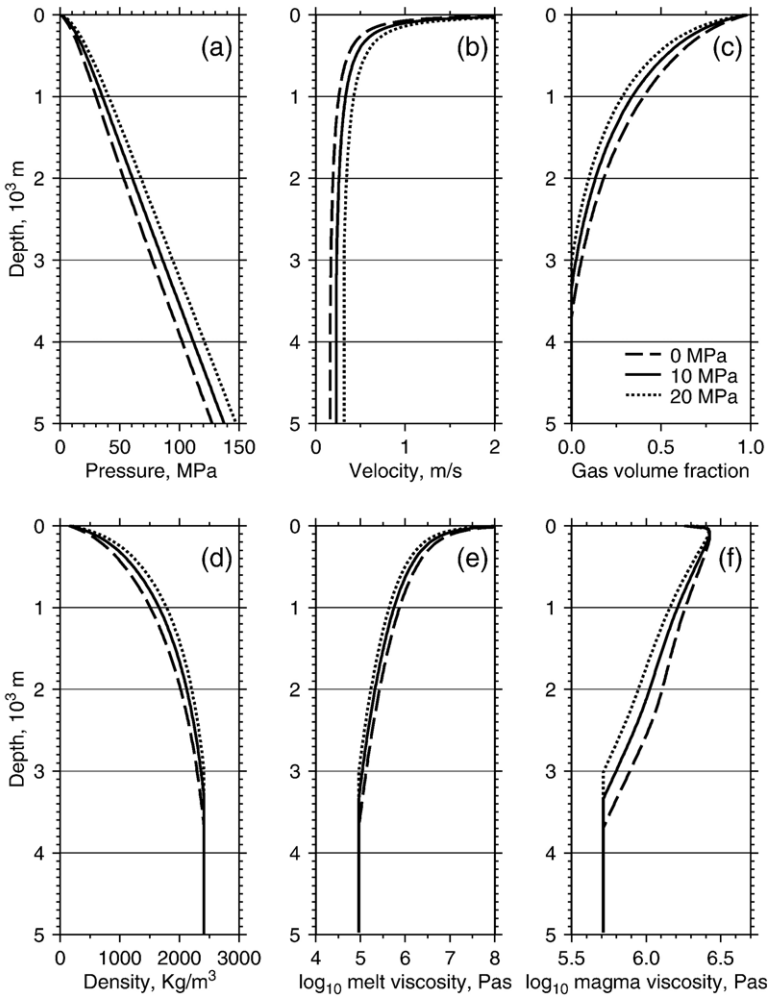

Fig. 3. Depth variation of magma properties (a) Pressure with P_{ch}=0/10/20 MPa as marked (r=0). (b) Maximum vertical velocity of magma. (c) Gas volume fraction which increases as depth and pressure decreases. (d) Resultant variation of magma density (Eq. (4)). (e) Melt shear viscosity and (f) Bulk magma shear viscosity including the effects of crystals and bubbles. All input parameters are listed in Table 1.

develop altering the overall flow behaviour of magma. The Finite Element Method conduit flow models of Massol et al. (2001) observed these variations and showed how flow velocity, for example, is altered by including compressibility.

The 2D conduit flow model developed within this paper illustrates that lateral pressure variations develop, with the pressure less at the walls than at the centre. However, this only occurs in the upper 1000 m due to the increased 14 flow velocities, as found by Massol et al. (2001). In general, as the flow velocity increases the lateral parameter variations become more prominent. At the exit of the cylindrical conduit, the lateral pressure variation is around half the pressure at the centre of the conduit.

These lateral pressure variations cause other magma properties to vary across the conduit, e.g. gas volume fraction and viscosities. Due to the variation in pressure, gas bubbles form preferentially close to the conduit walls, rather than within the centre of the flow. Correspondingly the shear viscosity of the melt is observed to increase rapidly as the conduit walls are approached (Fig. 4), as here the amount of water dissolved in the melt (c_m) decreases (Eq. (6)). However, due to the effect of the bubbles, which are elongated in such a flow (C_a>1), the magma shear viscosity displays the opposite behaviour, decreasing as the conduit wall is approached, due to the increased gas volume fraction in this region. These differences between the melt and magma shear viscosities, displayed here (Fig. 4) and in the previous section (Fig. 3), indicate that assuming the shear viscosity of the magma can be represented by the melt shear viscosity would greatly alter flow dynamics and therefore, the overall state of magma at depth.

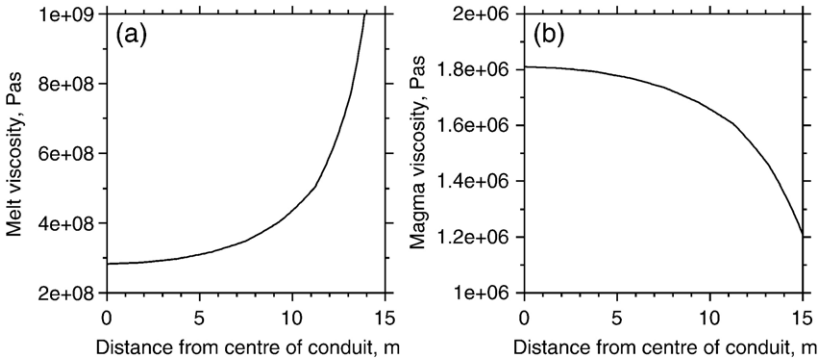

Fig. 4. Variations of (a) melt shear viscosity and (b) magma shear viscosity with radial position at the conduit exit ($z=0$ m). The lateral pressure changes causes gas bubbles to form preferentially at the wall, reducing the magma shear viscosity, and decreasing the dissolved water content, increasing the melt shear viscosity.

These results indicate that modeling conduit flow in 1D oversimplifies the problem, especially at shallow depths, as the horizontal variations in pressure, and hence the variation in other magma parameters are neglected, causing the overall flow characteristics to be altered. These results compliment those of Massol and Jaupart (1999) and Massol et al. (2001), and demonstrate the importance of modeling conduit flow in two-dimensions including magma compressibility.

3. Validity of isothermal assumption

Isothermal conditions are used in a number of conduit models, and are valid if the horizontal conductive heat flux into the surrounding country rock is negligible compared to the vertical convective heat flux (Woods, 1995). For the majority of the magma this can be assumed. However, in a small layer adjacent to the conduit wall, horizontal heat flux and cooling of the magma cannot be considered to be negligible (Bruce and Huppert, 1990; Stasiuk et al., 1993). This thin layer of cooled magma next to the conduit wall is referred to as the *Thermal Boundary Layer* (TBL), and must be considered when modeling magma flow in 2D.

In a magma conduit, due to the low thermal conductivities of melt (Murase and McBirney, 1973) the TBL is expected to be small, though the degree by which the magma within this region is cooled is unknown. The shear viscosity of the melt is known to depend on temperature (Hess and Dingwell, 1996) and would therefore, be greatly affected by such cooling near the conduit walls, possibly affecting overall flow dynamics. To gain insight into the magnitude of cooling within the magma conduit, simplified 1D heat flow models are solved numerically using a Finite Element Method (FEM). Heat sources due to friction and chemical processes are neglected.

The width of the TBL (Thermal Boundary Layer) is estimated by considering flow along a plane boundary (Bird et al., 2002). This approximation is reasonable as the diameter of a magma conduit is large in comparison to the expected width of the TBL (δ_T). For simplicity a magma is considered with a constant gas volume fraction of 30% and therefore, a constant magma density 16 (Eq. (4)). The width of the TBL for such a magma is 0.3–0.5 m (parameters as in Table 1). The TBL is therefore, only 3% of the conduit radius ($a=15$ m), and hence, it can be assumed that to the first order the isothermal assumption is valid.

To estimate the degree of cooling within this thin TBL the temperature of the conduit wall is determined. By applying the *no slip* boundary condition at the wall the vertical velocity of flow within the TBL is negligible, i.e. $v \approx 0$ m s^{-1}, for $r \geq a - \delta_T$. In the TBL, therefore, there is no vertical heat flux due to magma transport and the problem can be reduced to 1D conduction heat flow across the conduit wall in the r direction (Fig. 5). The initial temperature of the TBL and the constant temperature of the bulk of the magma conduit is taken to be 1100 K, and the initial temperature of the country rock is taken to be 273 K (0 °C). The system was simulated for 20 years, representing the length of time a magma conduit has been emplaced.

The variation of the temperature difference between the magma temperature and the cooled wall temperature (ΔT) with magma emplacement time is shown in Fig. 6. Once the magma has been emplaced within the conduit for around 5 years ΔT remains relatively constant within the range of 50–200 K, depending on the thermal conductivity assumed. These 1D models are representative of the degree of cooling felt within the

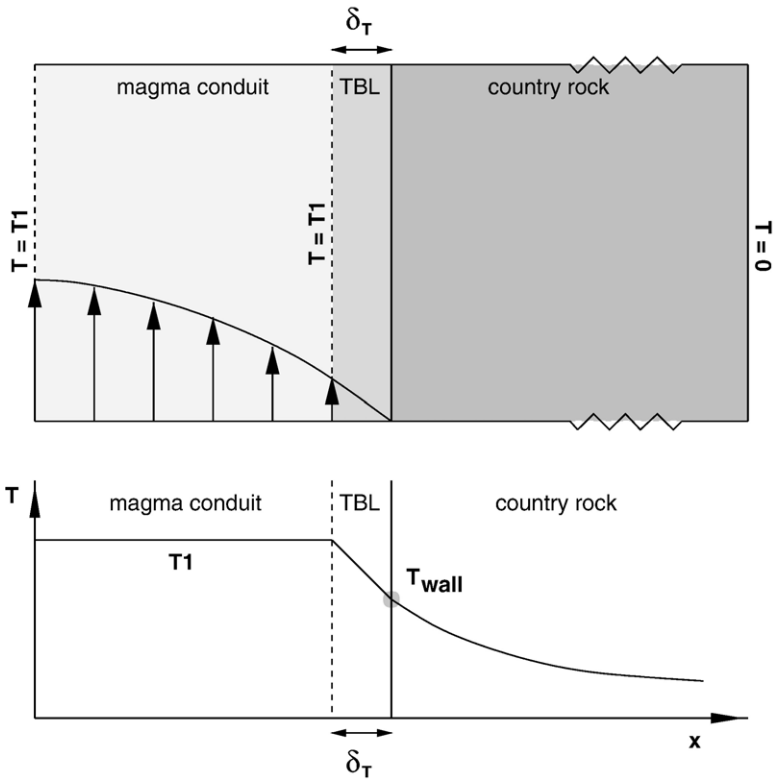

Fig. 5. Model set-up (top) with a sketch of how the temperature varies with horizontal distance, x, across the conduit wall (bottom). Here TBL is the Thermal Boundary Layer, of thickness δ_T.

TBL of a conduit with dyke geometry. For a cylindrical conduit (Fig. 2), the effect of the curved conduit wall boundaries would act to increase the degree of cooling, increasing ΔT. Therefore, from the results of these simple models, the difference between the magma and wall temperature is estimated to lie within the range 100–200 K.

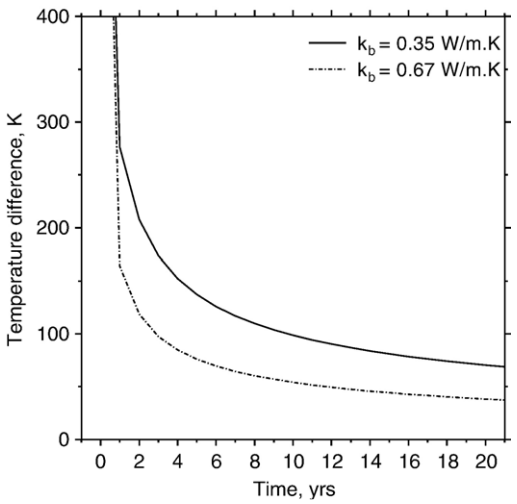

Fig. 6. Variation of $\Delta T = T_{magma} - T_{wall}$ with time of magma emplacement in years. Two magma thermal conductivities are used to illustrate the bounds of possible magma behaviour (Table 1).

This 100–200 K decrease in temperature within the TBL leads to a substantial increase of the melt shear viscosity (Hess and Dingwell, 1996). If magma is taken to have a dissolved water concentration of $c_m = 0.02$ (around 1000 m depth) the shear viscosity of the melt at the conduit wall will be at least one order of magnitude greater than that at the centre of the conduit with $\Delta T = 100$ K, and up to three orders of magnitude greater with $\Delta T = 200$ K. The estimated width of the TBL is however small (only around 0.4 m) compared to the conduit radius $a = 15$ m. Therefore, the decrease in temperature in this TBL, and corresponding increase in melt shear viscosity, has a small effect on the overall flow dynamics of the magma. Hence, it can be concluded that the effect of cooling within the thin TBL can be reasonably neglected when determining overall flow characteristics. However, this distinct, and sharp, variation of melt shear viscosity close to the conduit walls must be considered when investigating local processes occurring close to the conduit wall, such as brittle failure of melt.

4. Brittle failure of melt

Melt under certain conditions, called *glass transition*, has a viscoelastic rheology and, depending on the timescale of stress, can behave as a fluid or a solid (Dingwell and Webb, 1990). At low temperatures, and for short stress timescales, melt is unable to flow and responds in a brittle–solid manner, leading to fracturing and cracking. Evidence for brittle fracturing of melt has been observed in a number of exposed conduit sections and dome material (Eichelberger et al., 1986; Rust et al., 2004; Stasiuk et al., 1996; Tuffen et al., 2003). Furthermore, Gonnermann and Manga (2003) modeled conduit flow 18 and magma conditions at depth, and showed that brittle failure of melt, or localised fragmentation as they termed it, can occur close to the walls in magma conduits.

In glass transition viscoelastic melt rheology can be described by the Maxwell model, with the relaxation timescale given by (Dingwell and Webb, 1990),

$$\tau = \frac{\eta_m}{\mu_m}, \tag{20}$$

where η_m and μ_m are the shear viscosity and elastic modulus of the melt, respectively. During magma flow within conduits conditions of glass transition are likely to be reached and therefore, depending on the timescale of stress perturbations, the melt could react in a brittle manner, and fracture or crack. The onset of the conditions of brittle failure can be identified to occur when the product of the melt shear viscosity (η_m) and the shear strain rate ($\dot{\varepsilon}$) is greater than the shear strength of the melt (σ_m), i.e. when (Papale, 1999),

$$\frac{\eta_m \dot{\varepsilon}}{\sigma_m} > 1. \tag{21}$$

Within the 2D conduit flow model this brittle failure ratio can be applied to determine where, and at what depths, brittle failure of melt could occur in magma conduits.

As in Gonnermann and Manga (2003) brittle failure of melt is observed to occur at depth in conduits close to the wall, where the shear strain rate and the melt shear viscosity is at a maximum (Fig. 7). Therefore, brittle failure occurs within the Thermal Boundary Layer (TBL) and would be affected by cooling within this region, due to the corresponding increase in melt shear viscosity.

The sensitivity of the 2D conduit flow models and the depth of brittle failure of melt to all input parameters, including the degree of cooling, is tested in a series of model runs. Each input parameter is varied within a range (Table 1) and the depth of brittle failure is recorded. As the depth of brittle failure is known to be highly dependent on the degree of cooling within the TBL, the sensitivity model runs are split into three groups with $\Delta T = 100$, 150 and 200 K (Fig. 8), respectively. The greater the degree of cooling within the TBL, the deeper within the volcanic conduit brittle failure is estimated to occur (Fig. 8). The depth of brittle failure turns out to be highly dependent on the degree of cooling within the TBL, varying by several hundred metres when the wall temperature is reduced by just 100 K (Fig. 8).

Another parameter which is found to have a significant effect on the depth of brittle failure is the shear strength of melt (σ_m). This parameter is not well constrained and varies over one order of magnitude for pure glass, 10^7–10^8 Pa (Tuffen et al., 2003). The lower the strength of melt, the more easily brittle fracture can occur (Eq. (21)), and hence, the deeper the failure depth. Further work is necessary, therefore, to constrain this value, and the effects of bubble and crystal inclusions must be explored, as their presence may cause stress accumulations that might substantially reduce the effective strength of the melt (Spieler et al., 2004),

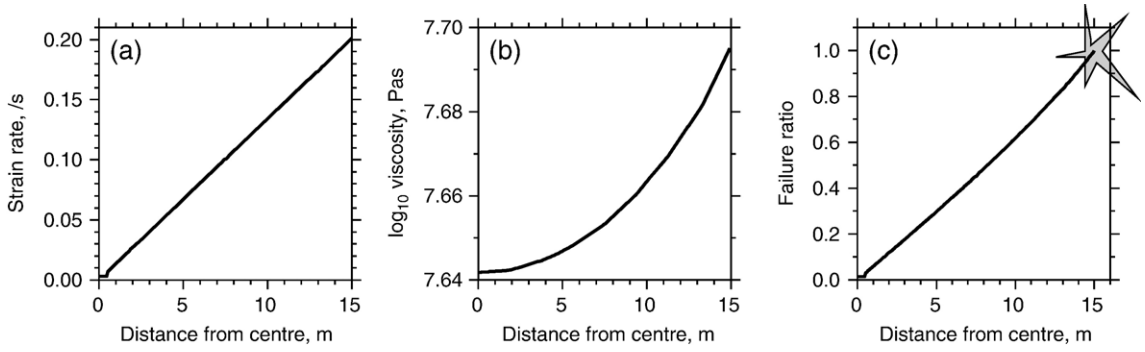

Fig. 7. Conditions for brittle failure: (a) variation of strain rate with radial position within the conduit, (b) variation of melt shear viscosity, and (c) resultant variation of brittle failure ratio (Eq. (21)), with the conditions for brittle failure met at $r = 15$ m.

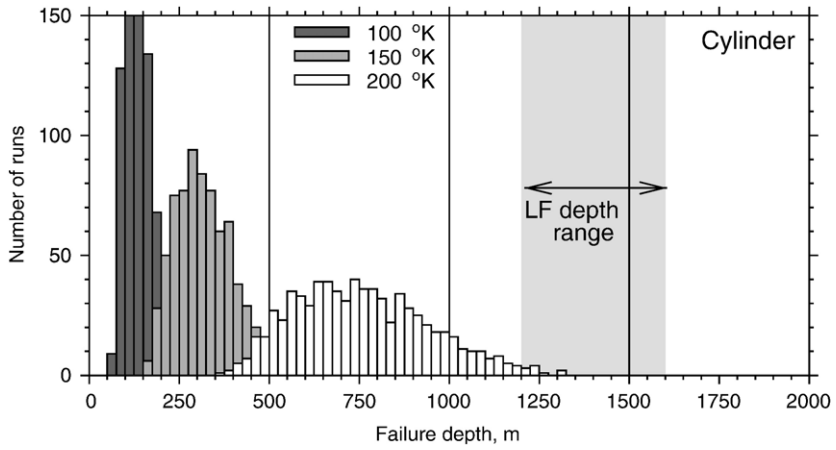

Fig. 8. Range of failure depths identified from sensitivity runs. In each case, a range of temperatures $\Delta T = 100/150/200$ K are shown. The greater ΔT the deeper the failure. The shaded area corresponds to the observed depths of LF events at Soufrière Hills Volcano (Fig. 9). Input parameters are taken at the minimum, maximum and middle values of the ranges in Table 1.

allowing brittle failure to occur more easily, i.e. under conditions of smaller melt viscosities and strain rates.

All other input parameters were found to have either a small effect, causing a change in the brittle failure depth of only 100 m or so, or are so well constrained by observations and experiments to not cause a significant variation in failure depth at all.

However, alternative mechanisms not taken into account within the conduit flow models developed here may also have a significant effect on the depth of brittle failure. For example, it is assumed in this model that the conduit radius is constant. It is likely that the magma conduit varies geometry (dyke to cylindrical pipe) or dimensions (widening or narrowing) with depth, which would act to alter the overall flow dynamics of the magma, and thereby, the depths at which brittle failure could occur.

In general, these results indicate that brittle failure of melt can occur in a localised region at depth within magma conduits. Furthermore, failure occurs close to the conduit wall within the Thermal Boundary Layer (TBL) and would therefore, be greatly affected by the degree of cooling felt within this region. The consequences of brittle failure of melt, specifically the formation of fractures and cracks, could affect the entire conduit flow dynamics and release seismic energy into the volcanic system.

5. Incorporating seismic observations

5.1. Observations of Low-Frequency (LF) events

Low-Frequency (LF) events are of great interest, as they seem to indicate the state of the volcanic system. Swarms of LF events have been observed to precede a number of volcanic eruptions, e.g. 1989–1990 eruption of Redoubt, Alaska (Stephens et al., 1994) and 1996 eruption of Soufri‘ere Hills Volcano, Montserrat (Miller et al., 1998). At Soufrière Hills Volcano, in particular, LF swarms correlate well with observed tilt signals (Voight et al., 1998; Green and Neuberg, in press), which, in turn, indicate the pressurisation and depressurisation of the volcanic system. These seismic events are, therefore, the key to further the understanding of processes occurring at depth in a volcano, and a greater knowledge of how these events are produced and formed would enable improved forecasting of future volcanic eruptions.

Characteristics of observed LF events at Soufri‘ere Hills Volcano provide the following clues regarding the attributes of the LF seismic energy source:

- LF events from 1995–1996 (Rowe et al., 2004) and from 1997 (Neuberg et al., in press) have been located beneath the active dome at a constant depth of 500 ± 150 m below sea level. Taking the height of the dome to be 1000 m above sea level (Watts et al., 2002), this corresponds to a depth of around 1500 m below the surface.
- LF events display highly similar waveforms and amplitudes (Green and Neuberg, in press; White et al., 1998), indicating a stationary common source mechanism, within a finite volume of 150 m × 150 m × 150 m (Neuberg et al., in press) (Fig. 9).
- The regular occurrence of LF events, within swarms, implies a highly periodic excitation by a repeatable, non-destructive source (Neuberg, 2000). Hence, any proposed LF seismic source must show these characteristics.

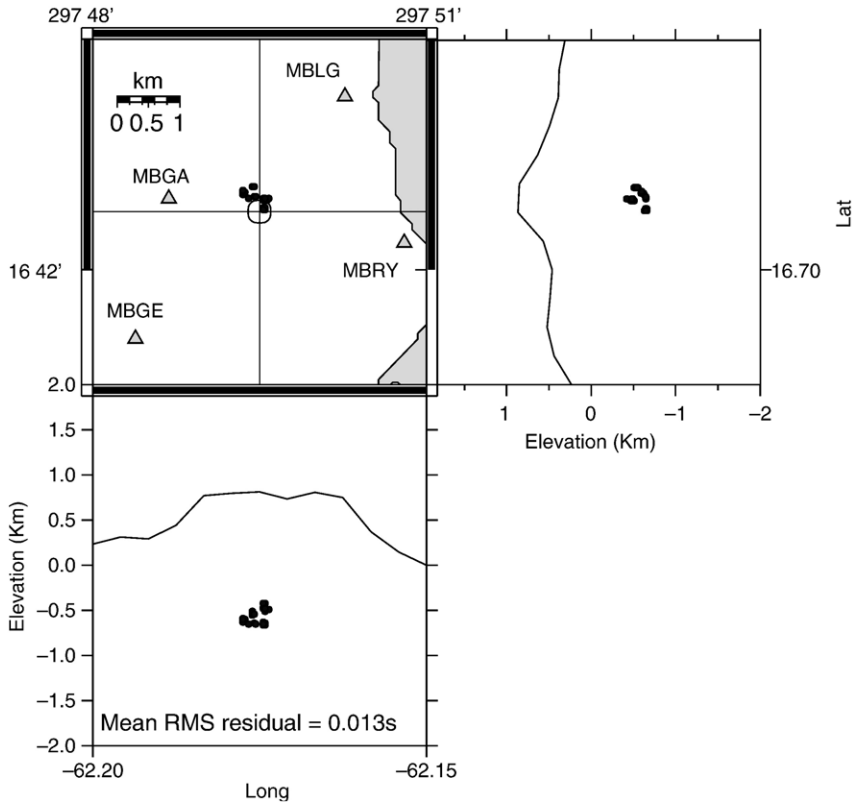

Fig. 9. Determined locations of LF events at Soufrière Hills Volcano in 1997. Residual rms converts to an error of 150 × 150 × 150 m. All events locate around 500 m b.s.l. Taken from Neuberg et al. (in press).

5.2. Brittle failure of melt as the LF seismic source

Brittle failure of melt within the magma conduit has been proposed to be a source of seismic energy at depth within silicic volcanoes (Goto, 1999; Tuffen et al., 2003). Brittle failure of melt may act as the LF seismic source (Neuberg et al., in press), possibly explaining the link between LF event occurrence and 22 magma movement at depth. As discussed in the previous section, for brittle failure of melt to act as the LF event source the key criteria determined from seismic observations must be satisfied.

To achieve brittle failure, according to the criterion $\eta_m \dot{\varepsilon} \geq \sigma_m$, at depths matching the observed LF location, around 1500 m, the temperature difference between the bulk of the magma and that at the conduit wall must be 200 K (Fig. 8). The deepest depth of brittle failure determined in a sensitivity analysis (using input parameters throughout their proposed ranges, see Table 1) is 1325 m, with $\Delta T = 200$ K. This expresses the importance of including cooling in a thin thermal boundary layer, and lateral parameter variations, when estimating brittle failure depth.

The strength of melt (σ_m) has also been shown to greatly alter the depths where the conditions of brittle failure are reached. In general, the shear strength of melt is not well constrained with estimates varying over one order of magnitude for pure glass (Tuffen et al., 2003). If we use the observed source depth of LF events as a constraint, an estimation for the strength of melt required to give brittle failure at this depth can be found. If all other parameters are taken at their mid-value within their ranges (Table 1), and assuming a failure depth of 1500 m, the strength of melt results in $\sigma_m = 4 \times 10^5$ Pa. This is substantially lower than the range estimated from pure melt (10^7–10^8 Pa). Though, whether the effect of including crystals and bubbles, localising stress, would lower the effective strength of melt by such a degree is unknown, and requires further experimental studies (e.g. Spieler et al., 2004).

As discussed previously, other mechanisms not tested within these conduit flow models could also affect the depth of brittle failure, and therefore, the 23 seismic source depth. If the magma conduit had an irregular conduit shape, with varying geometry and dimensions,

flow rates could be altered such that brittle failure conditions become localised at certain depths, creating a stable, stationary seismic source.

5.3. Incorporation into conduit flow models

Brittle failure of melt, specifically the formation of fractures and cracks, could affect the entire flow dynamics of magma within the conduit (e.g. pressure and velocity of flow) and therefore, the eruption style. Such fractures and brecciated regions at the conduit walls would allow open pathways for gas to escape (Gonnermann and Manga, 2003; Rust et al., 2004), and possibly allow the magma to slip at the walls in a friction-controlled manner.

For this reason the 2D conduit flow models are extended to include friction-controlled slip (Eqs. (17) and (18)) and gas loss (Section 2.1.1) at depths where the brittle failure criterion (Eq. (21)) is satisfied and fractures and cracks are formed. The conceptual model by Neuberg et al. (in press) suggests that this depth where cracks are formed by brittle failure of melt coincides with the trigger location of LF seismic events. As the magma is ascending, these cracks are pushed up within the rising magma, and fresh magma, now at the brittle failure depth, cracks and fractures. This process then results in a series of cracks lining the conduit walls at all depths at, and above, the identified depth of brittle failure. These cracks could then allow friction-controlled slip and gas loss to occur (Fig. 10). This slip is steady-state, and not stick-slip as applied within the model of Denlinger and Hoblitt (1999), and is therefore, fundamentally aseismic, causing no release of seismic energy. By including slip 24 and gas loss the magma ascent alters such that the seismogenic zone, i.e. the region where brittle failure occurs, remains at a constant depth.

By changing the boundary conditions at the conduit wall, from *no slip* to friction-controlled slip, from the brittle failure depth upwards, the dynamics of magma ascent within the conduit are altered. The velocity of magma at the conduit wall becomes non-zero, and correspondingly the velocity in the centre of the conduit decreases to conserve mass (Fig. 11(a)). This acts to decrease the shear strain rate of the magma flow at the depths above brittle failure, reducing the likelihood that the conditions of brittle failure of melt are met at shallower depths (Fig. 11(d)). This implies that as brittle failure occurs, producing cracks and fractures, friction-controlled slip and gas loss can occur within the conduit, no further fracturing at shallower depths would take place and the magma ascent would be aseismic.

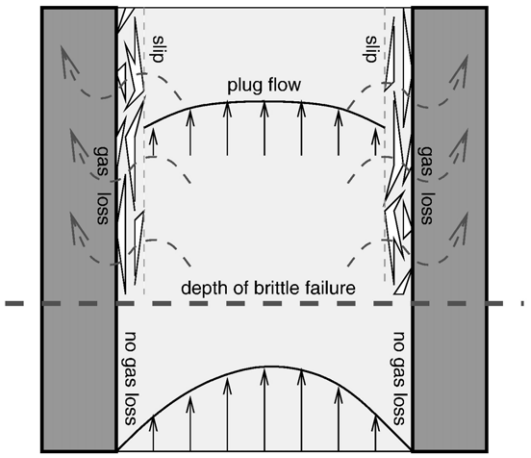

Fig. 10. Sketch of magma flow within a conduit. Below the melt brittle failure depth the conduit is 'closed' and at the wall the *no slip* boundary condition is applied. Whereas, at, and above, this depth the fractured and brecciated region allows flow at the wall, friction-controlled slip, and gas to be lost from the magma.

Including such a sudden loss of gas within the conduit causes a large and sudden change in the density of magma and other parameters, such as shear and volume viscosities of the magma (Fig. 11(b) and (c)). At the brittle failure depth, and immediately above it, the sudden loss of gas results in a dense, viscous magma region changing the velocity and pressure of the magma as it ascends (Fig. 11). As the velocity of the magma above the failure depth becomes reduced as gas is lost, due to mass conservation, the shear strain rate is also reduced reducing the likelihood of further brittle failure and allowing the magma to rise aseismically.

By including gas loss the exit gas volume fractions are greatly reduced compared to the original *closed* conduit models (Section 2.3). This decreases the magma ascent rates compared to the *closed* conduit models, such that the average extrusion rate is reduced to 0.16, around the range observed at Soufrière Hills Volcano, Montserrat (0.01–0.1 m s^{-1}; Watts et al., 2002).

By including friction-controlled slip and gas loss the fundamental flow of magma is altered and causes the identified depth of brittle failure of melt to drop deeper in the conduit. For example, a model run not including friction-controlled slip or gas loss has a brittle failure depth of 452 m, whereas including such processes and mechanisms the depth of brittle failure drops to 830 m.

As discussed, the act of brittle failure of melt may cause friction-controlled slip and gas loss. However, it is unknown how the flow of gas and ash through cracks

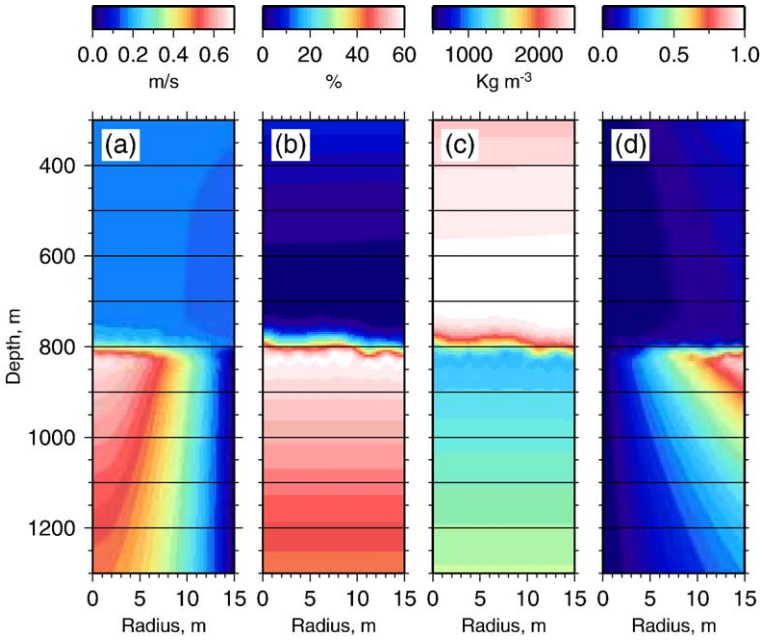

Fig. 11. Variation of parameters with depth and lateral position in the conduit shown in colour, at 830 m brittle failure occurs and friction-controlled slip and gas loss are included. (a) Velocity of flow, above the brittle failure depth plug-like flow develops, reducing the shear strain rate. (b) Variation of gas volume fraction (%), above the brittle failure depth gas is lost from the system. (c) The corresponding variation in magma density, affected by the gas loss above 830 m depth. (d) Brittle failure ratio, illustrating that brittle failure conditions (>1) are reached at one depth location within the conduit. Input parameters are given within the parentheses of Table 1.

or brecciated regions created by brittle failure affects the conditions of friction and slip. It is possible that such a flow would act to lubricate and unlock the magma from the wall and facilitate aseismic slip (Brodsky and Kanamori, 2001; Rust et al., 2004). Furthermore, conditions may arise such that no slip could occur at the conduit walls, or a stick-slip motion occurs (Denlinger and Hoblitt, 1999). (Gonnermann and Manga, 2003) studied the effect of brittle failure on magma flow considering no slip at the walls. They proposed that the brittle failure caused localised fragmentation, possible producing seismic energy, and that above the fragmentation point the viscous flow of magma allowed the cracks and fractures to flow, re-attach and reanneal forming flow bands. If conditions for stick-slip are met, it is possible that such a process could also produce seismic energy, independent of the brittle failure creating shear zones, though whether this source would satisfy the attributes of the LF seismic source is, as yet, unknown. In general, further work is required to investigate the effects of brittle failure at the conduit wall on boundary conditions, gas loss and therefore, on magma ascent. Also the effects of varying conduit radius or geometry (dyke or cylindrical pipe) must be explored, as it has a strong affect on magma ascent dynamics and therefore, on brittle failure. Further work should also be done on incorporating a non-linear rheology of magma within the conduit models. An example of such a non-linear rheology is yield strength (Bingham fluid), as such a flow has a different flow behaviour and therefore, strain rates and brittle failure depths to the flows modeled here.

The results of the 2D conduit flow models illustrate clearly that, by including friction-controlled slip and gas loss, brittle failure can only occur within one single stable depth region. This produces a stationary source of seismic energy, as required to produce seismic events like LF events. Furthermore, due to magma flow, fresh magma would constantly be moved into this depth region, indicating the likelihood of this source acting as a repeatable source, producing events with similar waveforms. Hence, brittle failure of melt satisfies the required characteristics of the LF event source.

6. Conclusions

In this study a 2D conduit flow model was developed that enabled magma properties to be resolved at all depths and lateral positions within the conduit. The 2D nature of these models allowed investigation into lateral parameter variations caused by the compressibility of flow and mechanisms which occur close to or at

the conduit wall, e.g. heat loss and brittle failure. The basic results of the conduit flow models clearly illustrate that neglecting the effect of gas bubbles on flow overestimates the viscosity of the magma and therefore, alters the overall flow dynamics.

By applying the 2D conduit flow models to exploring the process of brittle failure of melt, it was found that brittle failure, leading to cracking and fracturing, could occur at depth within magma conduits at localised regions close to the conduit wall within the thermal boundary layer. The conduit models were extended to include the consequences of brittle failure, namely friction- controlled slip and gas loss, and the results illustrated the substantial effect such processes have on the state of magma at depth and its ascent towards the surface. The simulations highlighted that once brittle failure occurs, friction-controlled slip and gas loss act to produce conditions where brittle failure exists at one stationary depth level, with aseismic magma ascent above this point. This illustrates that brittle failure of melt satisfies the characteristics of the LF event source, and could therefore, be key to understanding the underlying interaction between magma ascent and its state, and the occurrence and frequency of observed LF seismic events.

Acknowledgements

This work was funded by a University of Leeds research scholarship and by MULTIMO (EVGI-CT-2000-0002) which is supported by the Environmental and Sustainable Development Program of the European Commission Research Directorate General. Thanks to David Green for LF event location analysis and to the Volcano Seismology Group at the University at Leeds for many fruitful discussions. This paper was greatly improved by the comments and suggestions of the reviewers, Oleg Melnik and Hélène Massol.

References

Bagdassarov, N., Dingwell, D., 1993. Frequency dependent rheology of vesicular rhyolite. J. Geophys. Res. 98 (B4), 6477–6487.

Barclay, J., Rutherford, M., Carroll, M., Murphy, M., Devine, J., 1998. Experimental phase equilibria constraints on pre-eruptive storage conditions of the Soufrière Hills magma. Geophys. Res. Lett. 25 (18), 3437–3440.

Bird, R., Stewart, W., Lightfoot, E., 2002. Transport Phenomena, 2nd edition. John Wiley and Sons, Inc.

Brodsky, E., Kanamori, H., 2001. Elastohydrodynamic lubrication of faults. J. Geophys. Res. 106 (B8), 16367–16374.

Bruce, P., Huppert, H., 1990. Solidification and Melting in Dykes by the Laminar Flow of Basaltic Magma. Wiley.

Buresti, G., Casarosa, C., 1989. One-dimensional adiabatic flow of equilibrium gas–particle mixtures in long vertical ducts with friction. J. Fluid Mech. 203, 251–272.

Carmichael, R., 1990. Physical properties of rocks and minerals. CRC, pages 139 and 429.

Denlinger, R., Hoblitt, R., 1999. Cyclic eruptive behaviour of silicic volcanoes. Geology 27 (5), 459–462.

Devine, J., Murphy, M., Rutherford, M., Marclay, J., Sparks, R., Carroll, M., Young, S.J.G., 1998. Petrological evidence for pre-eruptive pressure–temperature conditions and recent reheating of andesitic magma erupting at Soufrière Hills Volcano, Montserrat, W.I. Geophys. Res. Lett. 25 (19), 3669–3673.

Dingwell, D., Webb, S., 1990. Relaxation in silicate melts. Eur. J. Mineral. 2, 427–449.

Dobran, F., 1992. Nonequilibrium flow in volcanic conduits and application to the eruptions of Mt. St. Helens on May 18, 1980, and Vesuvius in AD 79. J. Volcanol. Geotherm. Res. 49, 285–311.

Edmonds, M., Oppenheimer, C., Pyle, D., Herd, R., Thompson, G., 2003. SO_2 emissions from Soufrière Hills Volcano and their relationship to conduit permeability, hydrothermal interaction and degassing regime. J. Volcanol. Geotherm. Res. 124, 23–43.

Eichelberger, J., Carrigan, C., Westrich, R., Price, R., 1986. Non-explosive silicic volcanism. Nature 323, 598–602.

Gonnermann, H., Manga, M., 2003. Explosive volcanism may not be an inevitable consequence of magma fragmentation. Nature 426, 432–435.

Goto, A., 1999. A new model for volcanic earthquakes at Unzen Volcano: melt rupture model. Geophys. Res. Lett. 26 (16), 2541–2544.

Green, D., Neuberg, J., in press. Waveform classification of volcanic lowfrequency earthquake swarms and its implication. J. Volcanol. Geotherm. Res. 152. doi:10.1016/j.jvolgeores.2005.08.003.

Guèguen, Y., Palciauskas, V., 1994. Introduction to the physics of rocks. Thermal Conductivity. Princeton University Press. Ch. 10.

Hess, K.-U., Dingwell, D., 1996. Viscosities of hydrous leucogranitic melts: a non-Arrhenian model. Am. Mineral. 81, 1297–1300.

Hurwitz, S., Navon, O., 1994. Bubble nucleation in rhyolitic melts: experiments at high pressure, temperature, and water content. EPSL 122 (1–3), 267–280.

Jaupart, C., 1998. Gas loss from magmas through conduit walls during eruption. In: Gilbert, J., Sparks, R. (Eds.), The Physics Of Explosive Volcanic Eruptions. Special Publication-Geological Society of London, vol. 145, pp. 73–90.

Jaupart, C., Allègre, C., 1991. Gas content, eruption rate and instabilities of eruption regime in silicic volcanoes. Earth Planet. Sci. Lett. 102, 413–429.

Lahr, J., Chouet, B., Stephens, C., Power, J., Page, R., 1994. Earthquake classification, location, and error analysis in a volcanic environment; implications for the magmatic system of the 1989–1990 eruptions at Redoubt Volcano, Alaska. J. Volcanol. Geotherm. Res. 62, 137–151.

Lamb, H., 1945. Hydrodynamics, 6th edition. Dover Publications, pp. 586. Ch. XI.

Llewellin, E., Manga, M., 2005. Bubble suspension rheology and implications for conduit flow. J. Volcanol. Geotherm. Res. 143, 205–217.

Llewellin, E., Mader, H., Wilson, D., 2002. The constitutive equation and flow dynamics of bubbly magmas. Geophys. Res. Lett. 29 (24).

Lyakhovsky, V., Hurwitz, S., Navon, O., 1996. Bubble growth in rhyolitic melts: experimental and numerical investigation. Bull. Volcanol. 58, 19–32.

Manga, M., Loewenberg, M., 2001. Viscosity of magmas containing highly deformable bubbles. J. Volcanol. Geotherm. Res. 105, 19–24.

Manga, M., Castro, J., Cashman, K., Loewenberg, M., 1998. Rheology of bubble-bearing magmas. J. Volcanol. Geotherm. Res. 87, 15–28.

Marsh, B., 1981. On the crystallinity, probability of occurrence, and rheology of lava and magma: contributions to mineralogy and petrology. Bull. Volcanol. 78, 85–98.

Massol, H., Jaupart, C., 1999. The generation of gas overpressure in volcanic eruptions. Earth Planet. Sci. Lett. 166, 57–70.

Massol, H., Jaupart, C., Pepper, D., 2001. Ascent and decompression of viscous vesicular magma in a conduit. J. Geophys. Res. 106 (B8), 16223–16240.

Mastin, L., 1995. A numerical profram for steady-state flow of Hawaiian magma–gas mixtures through eruptive conduits. USGS Open File Rep. 95-756 (44).

Mastin, L., Ghiorso, M., 2000. A numerical program for steady-state flow of magma–gas mixtures through vertical eruptive conduits. USGS Open File Rep. 00-209.

Melnik, O., Sparks, R., 1999. Nonlinear dynamics of lava dome extrusion. Nature 402, 37–41.

Melnik, O., Sparks, R., 2002. Dynamics of magma ascent and lava extrusion at Soufrière Hills Volcano, Montserrat. In: Druitt, T., Kokelaar, B. (Eds.), The Eruption of Soufrière Hills Volcano, Montserrat, From 1995 to 1999, Memoirs of the Geological Society of London, vol. 21, pp. 153–171.

Miller, A., Stewart, R., White, R., Luckett, R., Baptie, B., Aspinall, W., Latchman, J., Lynch, L.B.V., 1998. Seismicity associated with dome growth and collapse at the Soufriére Hills Volcano, Montserrat. Geophys. Res. Lett. 25, 3401–3404.

Murase, T., McBirney, A., 1973. Properties of some common igneous rocks and their melts at high temperatures. Geol. Soc. Amer. Bull. 84, 3563–3592.

Navon, O., Chekhmir, A., Lykhovsky, V., 1998. Bubble growth in highly viscous melts: theory, experiments, and autoexplosivity of dome lavas. Earth Planet. Sci. Lett. 160, 763–776.

Neuberg, J., 2000. Characteristics and causes of shallow seismicity in andesite volcanoes. Philos. Trans. R. Soc. Lond., A 358, 1533–1546.

Neuberg, J., Tuffen, H., Collier, L., Green, D., Powell, T., Dingwell, P., in press. The trigger mechanism of low-frequency swarms on Montserrat. J. Volcanol. Geotherm. Res. 152. doi:10.1016/j.jvolgeores.2005.08.008.

Papale, P., 1999. Strain-induced magma fragmentation in explosive eruptions. Nature 397, 425–428.

Papale, P., Dobran, F., 1993. Modeling of the ascent of magma during the plinian eruption of Vesuvious in A.D.79. J. Volcanol. Geotherm. Res. 58, 101–132.

Papale, P., Neri, A., Macedonio, G., 1998. The role of magma composition and water content in explosive eruption: 1. Conduit ascent dynamics. J. Volcanol. Geotherm. Res. 87, 75–93.

Prud'Homme, R., Bird, R., 1978. The dilational properties of suspensions of gas bubbles in incompressible Newtonian and non-Newtonian fluids. J. Non-Newton. Fluid Mech. 3, 261–279.

Rivers, M., Carmichael, I., 1987. Ultrasonic studies of silicate melts. J. Geophys. Res. 92, 9247–9270.

Rowe, C., Thurber, C., White, R., 2004. Dome growth behaviour at Soufrière Hills Volcano, Montserrat, revealed by relocation of volcanic event swarms, 1995–1996. J. Volcanol. Geotherm. Res. 134, 199–221.

Rust, A., Cashman, K., Wallace, P., 2004. Magma degassing bu ered by vapor flow through brecciated conduit margins. Geology 32 (4), 349–352.

Rutherford, M., Gardner, J., 2000. Rates of magma ascent. In: Sigurdsson, H. (Ed.), Encyclopedia of Volcanoes. Academic Press, pp. 201–217.

Shaw, H., 1974. In: Hofmann, A., Giletti, B., Yoder, H., Yund, R. (Eds.), Geochemical Transport and Kinetics. Carnegie Instiution of Washington, Ch. Di usion of Water in Granitic Liquids: Part 1. Experimental Data, pp. 139–172.

Sparks, R., 1997. Causes and consequences of pressurisation in lava dome eruptions. Earth Planet. Sci. Lett. 150, 177–189.

Sparks, R., Murphy, M., Lejeune, A., Watts, R., Barclay, J., Young, S., 2000. Control on the emplacement of the andesite lava dome of the Soufrière Hills Volcano, Montserrat by degassing-induced crystallization. Terra Nova 12, 14–20.

Spera, F., 2000. Physical properties of magma. In: Sigurdsson, H. (Ed.), Encyclopedia of Volcanoes. Academic Press, pp. 171–190.

Spieler, O., Kennedy, B., Kueppers, U., Dingwell, D., Scheu, B., Taddeucci, J., 2004. The fragmentation threshold of pyroclastic rocks. Earth Planet. Sci. Lett. 226 (1–2), 139–148.

Stasiuk, M., Jaupart, C., Sparks, R., 1993. On the variations of flow rate in non-explosive lava eruptions. Earth Planet. Sci. Lett. 114, 505–516.

Stasiuk, M., Barclay, J., Carroll, M., Jaupart, C., Rattée, Sparks, R., Tait, S., 1996. Degassing during magma ascent in the Mule Creek vent (USA). Bull. Volcanol. 58, 117–130.

Stein, D., Spera, F., 1992. Rheology and microstructure of magmatic emulsions: theory and experiments. J. Volcanol. Geotherm. Res. 49, 157–174.

Stein, D., Spera, F., 2002. Shear viscosity of rhyolite-vapour emulsions at magmatic temperatures by concentric cylinder rheometry. J. Volcanol. Geotherm. Res. 113, 243–258.

Stephens, C., Chouet, B., Page, R., Lahr, J., Power, J., 1994. Seismological aspects of the 1989–1990 eruptions at Redoubt Volcano, Alaska: the SSAM perspective. J. Volcanol. Geotherm. Res. 62, 153–182.

Tuffen, H., Dingwell, D., Pinkerton, H., 2003. Repeated fracture and healing of silicic magma generates flow banding and earthquakes? Geology 31 (12), 1089–1092.

Voight, B., Hoblitt, R., Clarke, A., Lockhart, A., Miller, A., Lynch, L., McMa-hon, J., 1998. Remarkable cyclic ground deformation monitored in real-time on Montserrat, and its use in eruption forecasting. Geophys. Res. Lett. 25 (18), 3405–3408.

Watts, R., Herd, R., Sparks, R., Young, S., 2002. Growth patterns and emplacement of the andesitic lava dome at Soufrière Hills Volcano, Montserrat. In: Druitt, T., Kokelaar, B. (Eds.), The Eruption of Soufrière Hills Volcano, Montserrat, From 1995 to 1999, Memoirs of the Geological Society of London, vol. 21, pp. 115–152.

White, R., Miller, A., Lynch, L., Power, J., Sta, M.V.O., 1998. Observations of hybrid seismic events at Soufrière Hills Volcano, Montserrat, West Indies: July 1995 to September 1996. Geophys. Res. Lett. 25 (19), 3657–3660.

Wilson, L., Sparks, R., Walker, G., 1980. Explosive volcanic eruptions: IV. The control of magma properties and conduit geometry on eruption column behaviour. Geophys. J. R. Astron. Soc. 63, 117–148.

Woods, A., 1995. The dynamics of explosive volcanic eruptions. Rev. Geophys. 33 (4), 496–530.